Contents

1 Scientific, Technical, and Management Section

1.1 Observables and Baselines

We are proposing to study a probe-scale mission to extract the wealth of cosmological information contained in the spectrum and polarization of the cosmic microwave background (CMB). This information is unique and can not be provided through any other astrophysical observable.

The best measurements of the CMB spectrum – made by COBE/FIRAS approximately 25 years ago – show that the average CMB spectrum is consistent with that of a blackbody to an accuracy of 4 parts in 10^4 [30, 31]. Distortions in this spectrum encode a wealth of new information. The distortion shapes are commonly denoted as μ- and y-types. The μ-distortion arises from energy release in the early Universe and can only be produced in the hot and dense environment present at redshifts $z \gtrsim 5 \times 10^4$. This makes μ-distortions a unique messenger from a red-shift range that is not accessible to other probes. The y distortion is caused by energy exchange between the CMB photons and free electrons through inverse Compton scattering [35, 36]. These are caused at lower redshifts and are sensitive to the evolution of the large scale structure.

Thomson scattering at the surface of last scattering is the source of the polarization of the CMB. The polarization field can be decomposed to two modes that are independent over the full sky, an E and B-modes. Scalar perturbations, such as primordial energy density perturbation only give E-modes. The B-mode is a unique probe of early Universe tensor perturbations, such as Inflation [10, 11].

The starting points for our study are two missions, EPIC-IM and Super-PIXIE [**? ?**]. EPIC-IM was presented to the 2010 decadal panel as a candidate CMB polarization space mission. It is based on a 2 m aperture telescope and 11,094 bolometric transition edge sensors. Table **??** gives the mission's frequency bands and sensitivities. PIXIE is a proposed Explorer scale mission to measure the spectrum and polarization of the CMB. Super-PIXIE is a scaled up, much more capable version of PIXIE.

1.2 Science Objectives

1.2.1 Cosmic inflation

Inflation [1, 2, 3, 4, 5], a primordial era of accelerated expansion, provides a compelling dynamical origin for the observed statistical homogeneity of our universe on even the largest scales. Inflation dramatically smoothes away classical inhomogeneities, leaving the inevitable quantum fluctuations of the matter fields and the space-time metric during inflation as the source of structure today. The predictions of inflation are consistent with an impressive array of observations, including the CMB temperature and E-mode polarization and many surveys of the large scale structure of the universe at later times [6, 7, 8, 9]. But, inflation also predicts an as yet unobserved spectrum of primordial gravitational waves sourced directly by quantum fluctuations of the tensor component of the metric.

Figure 1 shows the predicted spectrum, current upper limits and measured B-modes from lensing, as well as forecasts for the EPIC-IM satellite. **should we put Planck E-modes on here?** The large-scale information provided by a satellite mission is complementary to the smaller scales accessible from the ground. For testing inflation, the largest scales are particularly important: only a satellite can demonstrate the presence of B-mode correlations on scales that were super-horizon at the time of recombination [24]. In addition, new tests of isotropy on the largest scales can only come from the reionization bump in the E-mode polarization [] and may contain information about the beginning of inflation. In its recent report New Worlds New Horizons (NWNH), the decadal survey committee strongly endorsed sub-orbital searches for the B-mode signal from inflation say-

ing that "The convincing detection of B-mode polarization in the CMB produced in the epoch of reionization would represent a watershed discovery." [12].

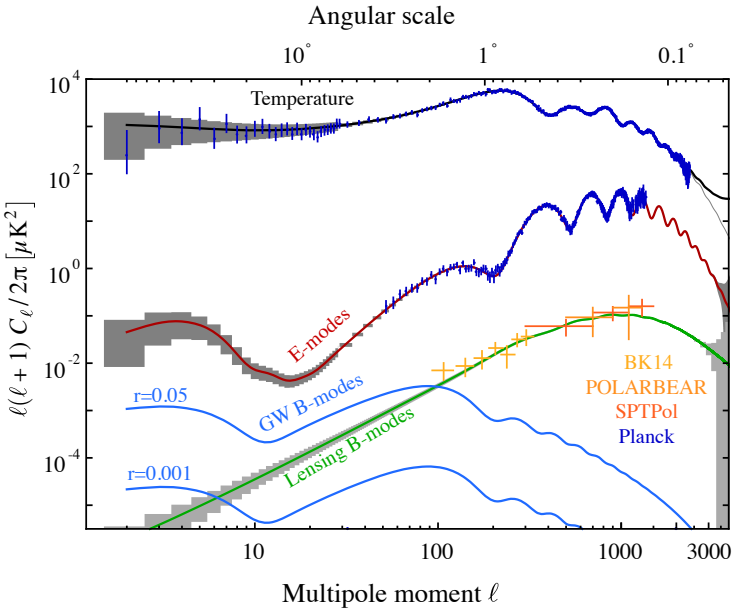

Figure 1: Theoretical predictions for the temperature (black), E-mode (red), and tensor B-mode (blue) power spectra. Primordial B-mode spectra are shown for two representative values of the tensor-to-scalar ratio: $r = 0.001$ and $r = 0.05$. The contribution to tensor B modes from scattering at recombination peaks at $\ell \sim 80$ and from reionization at $\ell < 10$. Also shown are expected values for the contribution to B modes from gravitationally lensed E modes (green). Current measurements of the B-mode spectrum are shown for BICEP2/*Keck Array* (light orange), POLARBEAR (orange), and SPTPol (dark orange). The lensing contribution to the B-mode spectrum can be partially removed by measuring the E and exploiting the non-Gaussian statistics of the lensing.

The predicted amplitude of the B-mode signal depends on the nature of the scalar sector driving inflation. Measurements of the CMB temperature fluctuations can be used to relate the inflationary potential energy V to r, the ratio of the temperature quadrupoles produced by gravitational waves to those from density perturbations, at the peak of the spectrum by $V^{1/4} = 3.7 \times 10^{16}\ r^{1/4}$ GeV. The observation of a primordial gravitational wave background would generate a revolution in our understanding the origin of our universe and the nature of particle physics, including gravity, at and above the Grand Unification scale of 10^{16} GeV.

Although there are many proposed inflationary scenarios, when the slow-roll criteria is met ($\epsilon \equiv -\dot{H}/H^2 \ll 1$) there are just two observationally viable classes of models that naturally explain the value of the spectral index n_s (by requiring $n_{\rm s}(\mathcal{N}) - 1 \propto -\frac{1}{\mathcal{N}}$, where $\mathcal{N}$ is the number of e-folds between the scale n_s where is observed and end of inflation) [13, 14, 15]. One class is the set of monomial potentials, which contains many of the canonical inflation models (eg, a quadratic potential) and is already under significant observational pressure. If the error bars on the spectral index tighten by a factor of about 2, and the 95% C.L. upper limit on r is pushed to even ~ 0.01, all such models would be ruled out (see Figure 2.). The remaining class of natural models includes Starobinsky and Higgs inflation (which both have $r \sim 0.003$). A future mission capable of reaching $\sigma_r \sim \mathcal{O}(10^{-4})$ would provide significant constraints on nearly every currently favored

inflation model. The EPIC-IM configuration is forecasted to acheive $\sigma(r) \sim 4.8 \times 10^{-4}$ assuming $r = 0.01$ and no foregrounds. **This number is for "EPIC-2m" from CMBPol paper. Couldn't find the comparable number in the EPIC-IM report.**

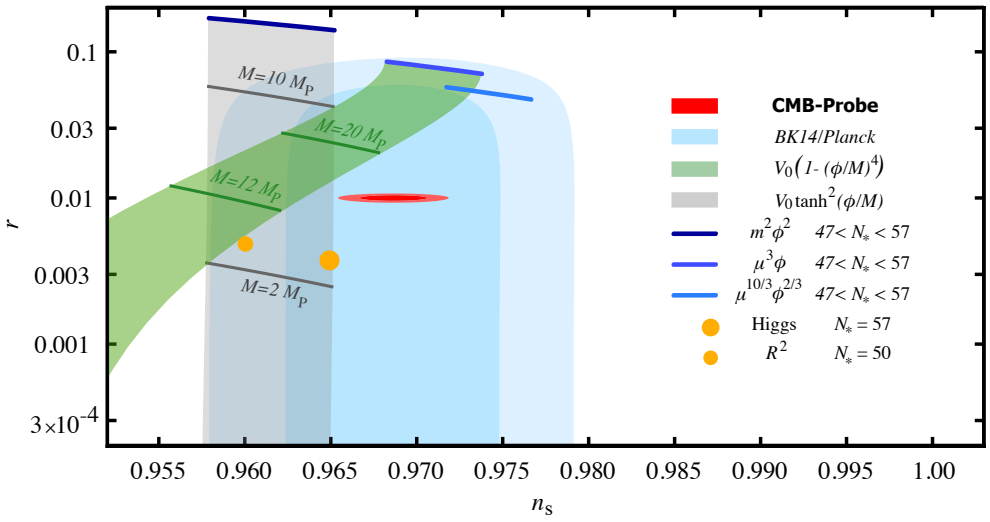

Figure 2: **Perhaps a version of this figure?** Forecast of CMB-S4 constraints in the $n_{\rm s}$–r plane for a fiducial model with $r = 0.01$. Constraints on r are derived from the expected CMB-S4 sensitivity to the B-mode power spectrum as described in Section **??**. Constraints on $n_{\rm s}$ are derived from expected CMB-S4 sensitivity to temperature and E-mode power spectra as described in Section **??**. Also shown are the current best constraints from a combination of the BICEP2/*Keck Array* experiments and Planck [**?**]. Chaotic inflation with $V(\phi) = \mu^{4-p}\phi^p$ for $p = 2/3, 1, 2$ are shown as blue lines for $47 < N_\star < 57$ (with smaller $N_\star$ predicting lower values of $n_{\rm s}$). The Starobinsky model and Higgs inflation are shown as small and large filled orange circles, respectively. The lines show the classes of models discussed in Section **??**. The green band shows the predictions for quartic hilltop models, and the gray band shows the prediction of a sub-class of α-attractor models [**?**].

Inflation generically predicts primordial gravitational waves just from the vacuum fluctuations of the metric during inflation, but of course does not preclude additional sources of B-mode polarization either during or after inflation. To be confident of the implications of a detection, the B-mode spectrum must be characterized. The vast majority of inflation scenarios predict a red spectrum for gravitational waves, and in the simplest cases the canonical single-field consistency relation fixes $n_{\rm t} = -r/8$. While confirming this relation is out of reach, a future satellite mission, combined with stage 3 ground based observations, could perhaps aim for $\sigma(n_{\rm t}) \lesssim 1$ to at least rule out non-vacuum inflationary sources [16, 17]. Post-inflationary phase transitions have been proposed as a non-inflationary source of nearly scale-invariant gravitational waves [18, 19, 20, 21, 22], but can be distinguished by the absence of super-horizon correlations at the time of recombination. A framework to extract specifically this part of the signal was proposed in Ref. [23] and could be applied to robustly extract the component of any signal that must come from physics outside of the hot big bang paradigm. Existing forecasts in the literature [24] indicate that a ground-based survey alone will not be able to detect super-horizon correlations at high significance if r is much below 0.1; a satellite will be required.

A detection of B-modes consistent with a primordial spectrum of vacuum fluctuations would be

the first observation of a phenomena directly related to quantum gravity. In addition, evidence for "large field" inflation would provide strong evidence that the complete theory of quantum gravity must accommodate a Planckian field range for the inflaton. The spectrum of tensor fluctuations depends only on the Hubble parameter H during inflation, while the scalar power depends on both H and the evolution of the homogeneous field sourcing inflation. As a consequence, the tensor-to-scalar ratio r determines the inflaton field range in Planck units (called the "Lyth bound" [25]) In many common inflationary models r is a monotonic function of $\mathcal{N}$ so that the tensor-to-scalar ratio at the CMB pivot point k_* is related to the distance the inflaton moves ($\delta\phi$) in Planck units by

$$\frac{\Delta\phi}{M_{\rm P}} \gtrsim \left(\frac{r_*}{8}\right)^{1/2} \mathcal{N}_* \gtrsim \left(\frac{r}{0.01}\right)^{1/2} . \tag{1}$$

The value of $\mathcal{N}_*$ is not well constrained and depends on unknown details of reheating, but $\mathcal{N}_* \gtrsim 30$ provides a conservative lower limit, justifying the second inequality in Eq. (1). Thus, a tensor-to-scalar ratio $r > 10^{-2}$ typically corresponds to a trans-Planckian excursion in field space between the end of inflation and the epoch when the modes we observe in the CMB exit the horizon. The relationship in Eq. (1) is significant because it relates the observed amplitude of linearized metric fluctuations to a property of the full quantum field theory for gravity coupled to the inflaton. The action describing inflation, like the action for any other particle physics phenomena, in general will include terms that encode the effects from degrees of freedom that couple to the inflaton, but are too energetic to be probed directly by physics near the inflationary scale. The field range is a measure of the distance in field space over which the corrections from the unknown physics do not significantly affect the low energy dynamics, since otherwise slow-roll inflation would not persist. In theories of quantum gravity we expect degrees of freedom to enter at the Planck scale or below. A field range exceeding the Planck scale would imply that quantum gravity contributions do not have a significant effect over the naively expected scale. A detection of r would therefore provide very strong motivation to better understand how "large-field inflation" can be naturally incorporated in quantum gravity.

Although the B-mode polarization is the richest source of new information, deeper mapping of E-mode polarization will also contribute to testing inflationary models. On the largest scales (accessible only from space), E-modes will provide new tests of isotropy, while on sufficiently small scales they will allow tighter constraints on the shape of the scalar power spectrum, the amplitude of scalar non-Gaussianities, and isocurvature modes.

In summary, a detection of primordial gravitational waves consistent with the standard inflationary prediction would reveal the presence of a new fundamental energy scale for particle physics and would have far reaching implications for quantum gravity. Detecting correlations on the largest scales would confirm a primordial origin. Any departure from a nearly scale-invariant, nearly Gaussian spectrum would reveal new physics beyond the simplest inflationary model. In the absence of a detection, an improvement by about two orders of magnitude on the current upper limit would qualitatively change how we think about the inflationary paradigm.

[DISTORTION PART DOES NOT LINK TO WHAT IS WRITTEN BEFORE YET. THE TEXT BEFORE HAS TO BE WORKED OVER SIGNIFICANTLY TO MAKE THAT MATCH.] Another clear target is predicted by the dissipation of small-scale perturbation through Silk-damping [53, 54, 55, 56]. This process allows us to place stringent constraints on the amplitude of the small-scale curvature power spectrum, present at scales (wavelength $0.1\,\mathrm{kpc} \lesssim \lambda \lesssim 1\,\mathrm{Mpc}$) and epochs ($10^4 \lesssim z \lesssim 10^6$) inaccessible through any other observation. It delivers a complementary test for the inflation paradigm [45, 57, 58, 59, 60], with $\mu = (2.0 \pm 0.14) \times 10^{-8}$ expected in ΛCDM [32]. Precise

measurements of signals at this level will be extremely challenging and requires unprecedented control of systematics and modeling of foregrounds. It would also bring us to the sensitivity level required to detect the cosmological recombination radiation [61, 62] imprinted by the recombination of hydrogen and helium at redshift $z \simeq 10^3 - 10^4$, which can be used to probe the physics of recombination. Anisotropy in the μ-distortion can furthermore be created through 'ultra-squeezed limit' non-Gaussianity [67, 68] and can be used to probe scale-dependent non-Gaussianity [69, 70]. Optimizing next-generation CMB spectrometers for these purposes requires extensive studies.

1.2.2 Neutrinos and Light Relics

After inflation, the universe was reheated to temperatures of at least 10 MeV and perhaps as high as 10^{10} GeV. At these high temperatures, even very weakly interacting or very massive particles can be produced in large abundances including those that would arise in extensions of the Standard model of particles physics. As the universe expands and cools, these particles will fall out of equilibrium and can leave observable signatures in, for example, the primary CMB and/or through gravitational lensing. Through these effects, the CMB is a very sensitive probe of neutrinos and their mass and many hypothetical light particles.

Much of the information about our thermal history and the particle content of the universe is encoded in the T and E power spectra. A high-precision measurement of these spectra over the full sky is expected to significantly improve our understanding of the post-inflationary universe. This is particularly true in E-mode polarization where, to date, far fewer modes have be measured at the level of cosmic variance than in temperature.

The spectra at high-ℓ contain important information about the components of the thermal plasma and their interactions around the time of recombination. One particular compelling target is the effective number of neutrino species, $N_{\rm eff}$, which parameterizes the total amount of energy density in radiation at the time of recombination. It is defined such that in the Standard model of particle physics with normal thermal evolution, $N_{\rm eff} = 3.046$ due to the energy density in the three species of neutrinos. $N_{\rm eff}$ is also sensitive to any additional light relic particles as their gravitational influence is identical to the neutrinos. In fact, if there was an additional light particle in thermal equilibrium with the Standard model particles at any point in our history, it will contribute a change to $N_{\rm eff}$ of at least $\Delta N_{\rm eff} \geq g\,0.027$ where $g \geq 1$ is the number of degrees of freedom of the new particle. This defines a compelling target of $\sigma(N_{\rm eff}) < 0.027$ for future CMB observations. New light particles are a common feature of many approaches to beyond the Standard model physics and can be directly tied to some of the most significant problems in the Standard model. Either a limit or detection of $\Delta N_{\rm eff}$ at this level would provide a powerful insight into the laws of nature and our thermal history.

The presence of free-streaming radiation changes the detailed features of the TT, TE and EE spectra at all ℓ. In particular, it changes the locations of the acoustic peaks and alters the damping tail at high-ℓ. Similar changes to the spectra arise from many other compelling targets including the helium fraction Y_p and more general dark sector physics. For this reason, constraints on $N_{\rm eff}$ a useful proxy for the information available in the high-ℓ power spectra.

Preliminary forecasts for $N_{\rm eff}$ are shown in the right hand panel of Figure 3. A space-based mission reaching an effective temperature noise of 1-2 μK-arcmin over the full sky gives competitive constraining power when compared other proposals. The two most important quantities for improving constraints on $N_{\rm eff}$ and other high-ℓ targets are $f_{\rm sky}$ and the temperature noise. The full-sky nature of the proposed mission would allow for cosmic variance limited E-modes over most of the sky and a large range of ℓ.

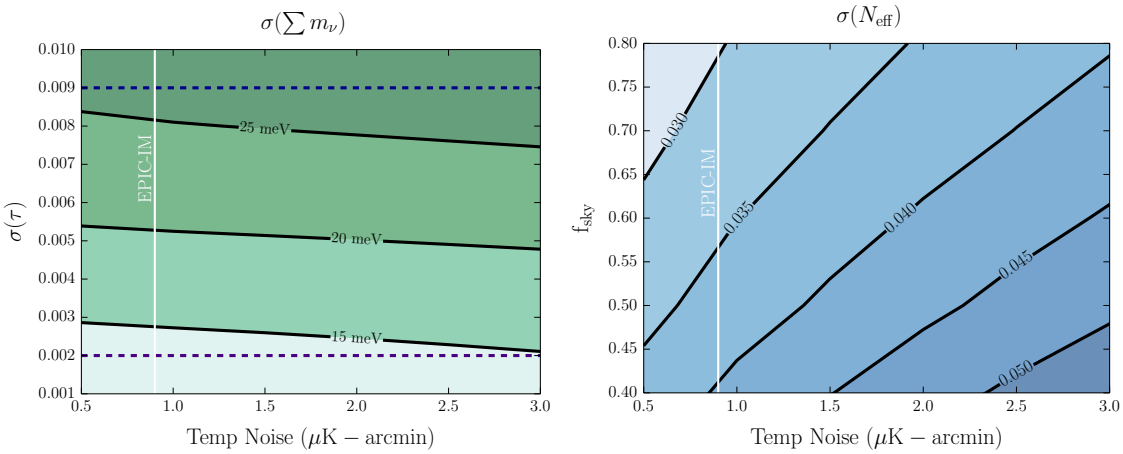

Figure 3: *Left:* Neutrino mass constraints as a function of the prior on τ for a 5' beam and sky fraction of $f_{\rm sky} = 0.7$. The blue dashed line is current Planck limit and the white dashed line a cosmic variance limit measurement of τ form the CMB. *Right:* $N_{\rm eff}$ Forecasts as a function temperature noise and sky fraction assuming 5' resolution.

The main downside of a space-based mission is that we cannot reach the resolutions available from the ground. However, we see that at 5' resolution and 1 μK-arcminute noise the forecasts are less sensitive to the resolution then one might naively expected. In particular we can reach $\sigma(N_{\rm eff}) < 0.035$ for temperature noise from 1-2 μK-arcmin and $f_{\rm sky} = 0.6 - 0.8$. These forecasts are competitive with CMB Stage IV. Specifically, the larger sky fraction and sensitivity available from space appears to compensate for the reduced resolution. In fact, the full sky measurement would provide complimentary information that could be combined with ground based surveys to further improve over the limits available from either experiment. This is particularly important for $N_{\rm eff}$ which is tantalizingly close to the target of $\sigma(N_{\rm eff}) = 0.027$ and therefore even an apparently modest improvement could have a major scientific impact.

The sum of neutrino masses, $\sum m_\nu$, is another theoretically compelling target that is accessible from Cosmology. The most distinctive feature of $\sum m_\nu$ is that it suppresses the growth of structure on small scales. This suppressed can be measure in the CMB through amplitude of the lensing power spectra compared to the primary CMB. In principle, this relative difference can yield a measurement of the minimum value of $\sum m_\nu = 58$ meV at 4-5 σ for a number of future cosmological surveys. However, sensitivity to $\sum m_\nu$ is ultimately limited by our knowledge of the primordial amplitude of fluctuations A_s which is strongly degenerate with the optical depth τ.

The current limit on τ from the Planck satellite of $\tau = 0.055 \pm 0.009$ ultimately limits $\sigma(\sum m_\nu) \gtrsim 25$ meV, as shown in the panel of Figure 3. While the figure shows the sensitivity of a space-based CMB mission to $\sum m_\nu$, this lower limit is common to any measurement that depends on the relative suppression. Therefore, a cosmological detection of $\sum m_\nu = 58$ meV at 3-5 σ depends crucially on an improvement measurement of τ. To date, the only proven method for such a measurement is from a space-based CMB observations. The best constraints on τ come from E-modes with $\ell < 20$ which requires control over the largest angular scales.

Measurements of the primary CMB and CMB lensing are very sensitive to particles with long-lifetimes that service until the era of recombination. Furthermore, the primary CMB is indirectly sensitive to BBN through the helium fraction, Y_p, that can be detect energy injections at those

times. However, many relics of the early universe are not cosmologically stable but can survive beyond the time of BBN. Energy injection between the two eras is not directly captured by the CMB anisotropies but can be tested by BBN consistency of Y_p with the measured value of $N_{\rm eff}$.

Additional, far more sensitive measurements of this intermediate era are possible through the *distortions* of the CMB black-body spectrum. This will allow us to place stringent bounds on the presence of long-lived decaying particles [43, 44, 45, 46] and other non-standard physics, such as axions, primordial magnetic fields and superconducting strings [e.g., 47, 48, 49, 50, 51].

1.2.3 Cosmological structure formation

Understanding the evolution of cosmological structures from the formation of the first stars to the present time is a key goal of cosmology [**?**]. The anisotropies in the Cosmic Infrared Background (CIB), produced by dusty star-forming galaxies (DSFGs) in a wide redshift range, are an excellent probe of both the history of star formation and the link between galaxies and dark matter across cosmic time. The *Planck* Collaboration [76, 77], derived limits on the star formation rate density that, at redshifts z~ 3, are about three times higher than constraints from number counts measurements ([78]). The new mission probe, by measuring CIB anisotropies with 100 times more sensitivity than *Planck*, will be able to shed light on this intriguing discrepancy, by strongly constraining the history of star formation in the range $0 < \mathrm{z} < 4$, and in particular with one tenth of the *Planck* uncertainty at z$= 3$. Moreover, it will be possible to identify and constrain a characteristic halo mass $M_{\rm eff}$, which determines the most efficient gas accretion and SFR, and therefore sets the evolution of the galaxies residing within a dark matter halo. Current models and measurements constrain this characteristic halo mass at $M_{\rm eff} \sim 10^{12}$ solar masses with about 10% uncertainty, while the new mission probe will constrain this parameter at the percent level.
Moreover, because DSFGs trace the underlying dark matter field in a broad redshift range, the CIB will correlate with multiple dark matter tracers such as catalogs of galaxies and quasars [79, 80], and diffuse maps of the γ-ray and the X-ray background [82]. These cross-correlations will provide an additional probe of the global star formation history, and they will shed light on the interaction between light and matter in a broad wavelength range.

Large-scale structure can also be probed using CMB spectral distortions measurements. In fact, the largest guaranteed distortion is caused by the associated late-time energy release of forming structures and from reionization [37, 38, 39, 40, 41], imprinting a y-type distortion with $y \simeq 2 \times 10^{-6}$ [e.g., 41, 42]. This distortion is only one order of magnitude below the current limit from COBE/FIRAS and, even with most pessimistic assumptions about foregrounds, should be clearly detected with the next-generation spectrometers we propose to study. A detection will give information about the total energy output of first stars, AGN and galaxy clusters. In particular, group-size clusters that have masses $M \simeq 10^{13}\,M_\odot$ contribute significantly to the signal. With temperature $kT_{\rm e} \simeq 1\,{\rm keV}$ these are still sufficiently hot to create a detectable relativistic temperature correction to the large y-distortion, which can be used to constrain the currently uncertain feedback mechanisms used in hydrodynamical simulations of cosmic structure formation [42]. These two inevitable signals probe the low-redshift Universe and provide clear targets for future spectral distortions measurements and their requirements in the presence of foregrounds.

The CMB spectrum varies spatially across the sky. One source of such anisotropic distortion is related to clusters of galaxies and has already been measured by Planck [63]. A combination of precise CMB imaging and spectroscopic measurements will allow observing the relativistic temperature correction of individual SZ clusters [64, 65, 66], which will calibrate cluster scaling relations and inform our knowledge of the dynamical state of the cluster atmosphere. Finally,

resonant scattering signals in the recombination [71, 72, 73] and post-recombination eras [74, 75] can lead to spectral-spatial CMB signals that can be used to constrain the presence of metals in the dark ages and the physics of recombination. For all these applications, instrumental synergies between CMB imaging and spectroscopy need to be studied in detail.

These studies will be key to address three of the seven key questions identified in the Astro2010 report "New Worlds, New Horizons in Astronomy and Astrophysics" (NAS Decadal Survey, p. 47): *What is the fossil record of galaxy assembly from the first stars to present? What are the connections between dark and luminous matter? How do cosmic structures form and evolve?*

1.2.4 Dark Matter

Characterizing the nature of dark matter is one of the most basic problems in cosmology and astroparticle physics. For a conventional WIMP candidate, the CMB places very stringent constraints on dark matter through possible energy injection at the time of recombination. A thermal relic will necessarily annihilate into Standard model particles which distorts the Thomson visibility function and ultimately the shape of the primary T and E spectra [**?** **?** **?**]. In principle, a dark matter candidate can also have a slow decay to dark matter particles which is similarly constrained by the CMB. **add citations**

A somewhat more model-independent approach is to constraint dark matter interactions that would effect the evolution of the effective dark matter fluid and its interactions with baryons or photons. The simplest example is to constraint the baryon-dark matter cross section through its effective coupling of the two fluids. These couplings effect the evolution of fluctuations and ultimately the T and E spectra. More exotic dark sectors can produce a rich phenomenology in the CMB and in the large-scale structure without necessarily producing an associated signature in direct detection experiments or indirect searches. **add citations**

Interactions of DM with standard model particles can also be constrained through CMB spectral distortions [52]. As the Universe expands, the matter cools. Compton interactions with electrons keep the normal matter at the CMB temperature until well after recombination. This leads to a small distortion of the CMB with a negative chemical potential [29]. In a similar manner, interactions of DM with electron, protons or directly with CMB photons can lead to a distortion. These constraints could be strongly improved with future CMB spectroscopy [52].

1.3 The Challenges: Foregrounds, systematics

3 pages. Discuss the challenge of Foregrounds and Systematics.

The search for primordial B-modes is one of the main science objectives of any future CMB mission. A satellite mission is the most sensitive probe of this signal from the early universe because it can access the full sky and the choice of frequencies is not limited by the atmosphere.

By the time of launch of a probe class mission substantial progress will already have been made. In the case of a detection at the time of launch, the probe mission should be able to convincingly detect the expected reionization signal. In the absence of a signal it should significantly improve the upper limits beyond $\sigma(r) = 0.001$.

The contribution from reionization to the Stokes Q-parameter for a tensor-to-scalar ratio $r = 0.001$ is shown in the left panel of Figure 4. The amplitude of the signal is approximately 10 nK so that any experiment attempting to measure such a signal must control foregrounds and systematics on large angular scales at an unprecedented level of a few nK.

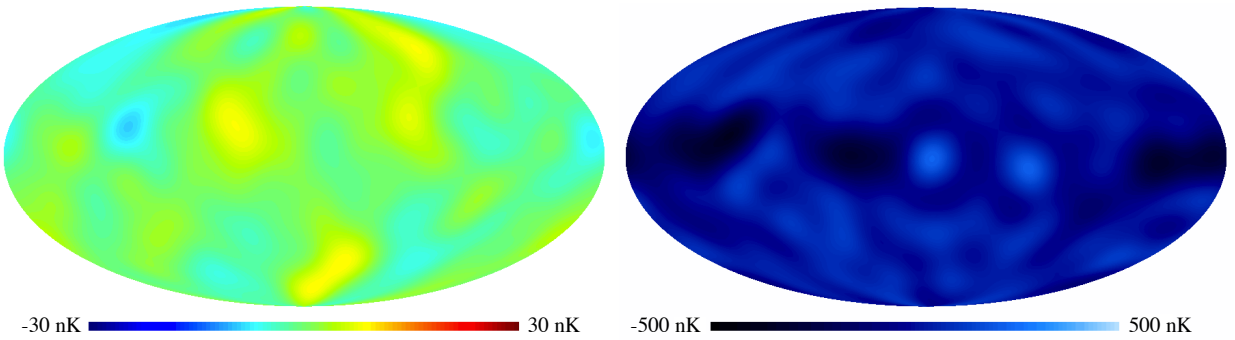

Figure 4: *Left panel:* Contribution to the Stokes Q parameter from inflationary B-modes for $\ell < 12$ for $r = 0.001$. *Right panel:* Noise in the $Planck$ 353 GHz map of the Stokes Q parameter for $\ell < 12$ rescaled to 150 GHz assuming the spectral properties of dust.

1.3.1 Foregrounds

Data from the $Planck$ satellite has significantly improved our understanding of foregrounds in both intensity and polarization. In polarization, the sky is dominated by the expected sources, synchrotron and dust, and $Planck$ has provided us with much improved measurements of their amplitude and spectral dependence. The observed spectral dependence is shown in the left panel of Figure 5 for different sky fractions. One of the most important lessons is that foregrounds are larger than putative primordial B-mode signal everywhere.

This is particularly severe on the scales relevant for the search of primordial B-modes as can be seen in the right panel of Figure 5, which shows the power spectrum of foregrounds over 75% of the sky for frequencies between 70 and 200 GHz together with the lensing and inflationary contribution for different values of the tensor-to-scalar ratio.

Perfect knowledge of the foreground components would allow to remove them, but the sensitivity of Planck limits our ability. The right panel in Figure 4 shows the noise in the $Planck$ 353 GHz map of the Stokes Q-parameter rescaled to 150 GHz assuming the same spectral dependence as for dust and on the angular scales relevant for the measurement of the inflationary B-modes. The noise is more than an order of magnitude larger than the inflationary contribution for $r = 0.001$, clearly indicating the necessity to measure foregrounds with a potential future space mission. A probe class mission likely is the only way to map foregrounds at a level required to measure primordial gravitational waves for $r < 0.001$.

While the search for primordial B-modes leads to the strictest constraints on foreground residuals, exquisit control of foregrounds is also necessary for other science objectives. A satellite mission is likely also the only reliable way to measure the optical depth at a level necessary to break the degeneracy with the neutrino mass. Furthermore, a cosmic variance limited measurement of E-mode polarization on large scales possible with a probe mission would contain valuable information about the star formation history.

Similarly, a clear objective of the spectral science is to have a robust, foreground-marginalized expectation of detecting the μ-distortion generated by the dissipation of small-scale acoustic modes in ΛCDM. While an instrument like PIXIE just falls short of this objective, it seems within reach of a probe mission.

One of the key ingredients in the design of a CMB experiment is the frequency coverage re-

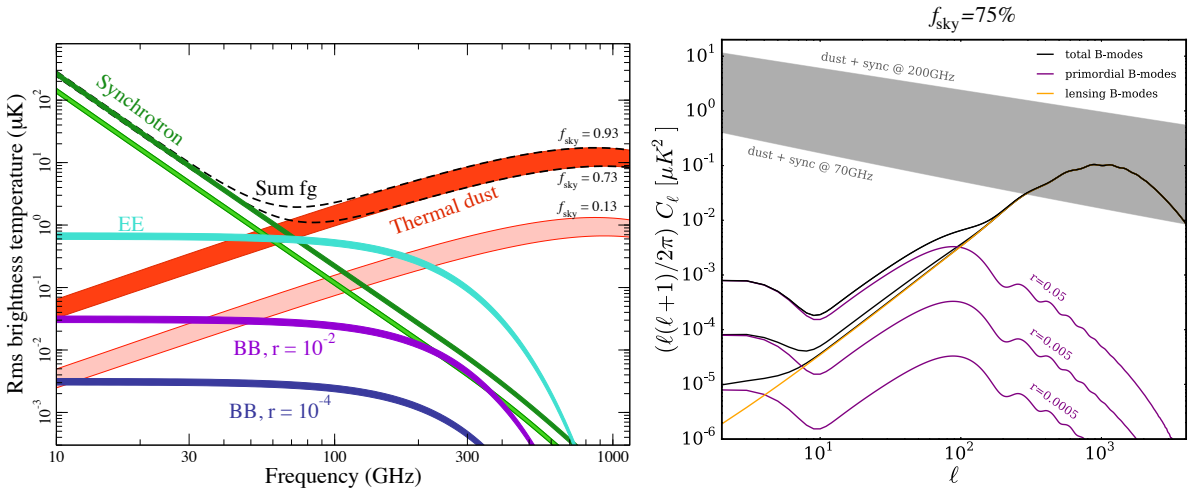

Figure 5: *Left panel:* Brightness temperature as function of frequency for the CMB as well as synchrotron emission (green) and dust emission (red). The darker bands show the brightness temperature for sky fractions between 73% and 93%, the lighter bands show the brightness temperature for the cleanest 13% with the width indicating the uncertainty. *Right panel:* Angular power spectrum for B-mode polarization of the CMB for $r = 0.0005$, $r = 0.005$, and $r = 0.05$ as well as for foreground emission between 70 and 200 GHz.

quired to achieve the science goals. Consequently, optimizing frequency coverage in light of the new information from $Planck$ and its limitations will be one of key task of the study proposed here.

1.3.2 Systematic Errors

Advances in detector technology since the formulation of Planck and WMAP will enable huge gains in raw sensitivity for a CMB probe. To fully take advantage of this sensitivity, systematic errors must be controlled to detect polarization signals at nano-Kelvin levels. The proposed study will invest heavily in designing an instrument, test plan, and observation strategy to address systematic errors, gathering decades of experience of ground-, balloon-, and space-based CMB polarimetry. The latest analyses of Planck HFI and LFI data in particular show the effects likely to be important to a future space mission(https://arxiv.org/abs/1605.02985). These systematic errors can be considered in three broad categrories: 1. Intensity-to-polarization leakage, 2. stability, and 3. straylight. Each of these is considered in light of differential polarimetery; the instantaneous signals measured by polarization-sensitive detectors at different times and orientations are combined to recover the maximum likelihood polarization signal from each point on the sky.

Leakage. The CMB temperature signal is many orders of magnitude larger than the polarization B-mode signal (see, e.g. Fig. 1). Therefore, instrumental mismatch effects that can leak even a very small fraction of an intensity fluctuation into a spurious polarization signal must be addressed. The main effects are relative gain and bandpass calibration, differential pointing error, and differential beam shapes.

Relative calibration requirements are likely to exceed those of Planck, whose High Frequency Instrument achieved of order 0.01% (cite https://arxiv.org/abs/1605.02985). Bandpass mismatch is the imperfect matching of the frequency dependant gain of the two detectors or acquisition channels used to estimate the polarized signal. Any asymmetry turns into a spurious polarization signal

when viewing sources with SED different from the calibrator. For CMB-probe, this includes every foreground contaminant on the sky. The effect can be minimized by matching the bandpasses, and residual mismatch can be estimated by measuring the bandpasses on the ground, however, for both instruments of Planck the ground based measurements of the bandpasses were found to be insufficient to determine the impact on the polarized maps. In both cases estimates of the bandpass mismatch needed to be determined as part of the mapmaking pipeline, and bandpass mismatch remains one of the most problematic systematics in the pipelines. CMB-probe will need a more robust program to mitigate this problem on ground, simulate the impact, and to deal with it in the flight data.

A second order complication of unmatched bandpasses is unmatched far sidelobe contamination, leading to a spurious polarized component from bright unpolarized signals far from the main lobe.

These systematics are likely to drive the instrumental requirements on the optical system as well as the uniformity of the bandpass of each polarimeter. Calibration requirements will also be set by limiting these systematics: particularly on the knowledge of the polarization parameters (such as cross-polar leakage and the angle of polarization sensitivity), as well as measurement of the beam shape (in general a function of the SED of the observed source). These systematic effects can potentially be mitigated by modulation of the sky signal in such a way that allows complete reconstruction of the polarized sky signal using each photometer, for example, using a half-wave plate.

Stability. Given the need to avoid light from the Sun, Earth, and Moon, the full reconstruction of the polarized sky will necessarily involve combination of measurements made at times seperated by months, requiring stability of the response of the instrument on corresponding time scales. This systematic error puts requirements on control of thermal drifts of spacecraft temperatures, to mitigate thermal emissivity changes and thermoelastic deformation of telescope structures. The cryogenic operating temperatures of detectors or reference calibration loads must be controlled adequately as well. Careful design of the scan strategy can shorten the time scales needed for stringent stability, for example Planck's scan strategy traced out great circles which overlapped on 1 minute timescales, giving a shorter effective time scale for stability requirements.

Additionally, the space radiation environment is modulated by the solar activity and can introduce drifts in the cryogenic thermal environment as well as introducing correlated transients in detectors and readout electronics. The design of the instrument must account this environment, which following Planck is much better understood.

Straylight. The brightest cm-wave and mm-wave sources in the sky (such as the Sun, Moon, planets, and Galactic center) passing into the far sidelobes of the telescope (defined as the response of a detector from a source more than a few degrees from the optical axis) in a sky-synchronous way can create a spurious polarization signal. he far sidelobe response can be reduced by the optical design and baffling, but will always be present at a non-trivial level. The Planck experience is instructive here as well. The detailed GRASP model of the telescope, convolved with the sky model, predicted sidelobe contamination at a visible (10's of microK) level in the 30 GHz maps, which was observed in difference maps. As a result the LFI maps have had an estimate of the sidelobe contamination removed from the timelines as part of the mapmaking process. The more stringent requirements for CMB-probe will necessitate at least this level of mitigation. A major limitation to the analysis of far sidelobe contamination in the Planck data has been the lack of bright enough on-orbit sources to validate the GRASP simlation as adjusted by optical and bandpass parameters estimated on-orbit. Finding a way to better validate the FSL model on-orbit for CMB-

probe may be critical to successfully removing FSL contamination.

1.4 Current and Forthcoming Efforts and the CMB Probe

2.5 pages. S3 experiments, forthcoming S4, Baselines CMB Probe options and their complementarity with S4.

Bill Jones is writing this. Due by Oct. 28

1.5 State of Technologies

2 pages. Discuss the technologies, their TRL, and what will be studied

A fourth generation CMB satellite targeting a map sensitivity of $\sim 1\mu\mathrm{k} - \mathrm{arcmin}$ will require, extremely sensitive detector arrays, tight control over systematics, and ability to reject polarized foregrounds as is described in Section 1.2. Given the frequency dependance of synchrotron and dust foregrounds, this last requirement translates into the need for a large number of spectral bands covering the approximate frequency range from $\sim$ 30 GHz to $\sim$ 800 GHz. Development of the CMB technologies needed to meet these requirements is actively being pursued by many groups who are also demonstrating these technologies on ground, balloon, and satellite platforms. We describe the status and needs in the areas of telescopes, optics, detector coupling, detectors, and readout.

Telescopes: Carbon Fiber Reinforced Polymer (CFRP) mirrors are at TRL 9 as they have flown on the Planck sattelite. Their 1.9x1.5 m mirror weighted only 28 lbs and met all surface quality requirements. However, small deformations in the mirror caused by its structural supports had a measurable impact to the beam far-sidelobes that was not caputred by preflight measurements or the corresponding beam modeling. Future CMB satellites will require improved pre-flight characterization of *polarized beam* at operating temperature augmented by improved simulation tools to meet even more systematics requirements. Current ground and balloon born optical designs achieve large field of views (FOVs) with reflective and refractive designs; related designs and their implementation should studied in the context of a satellite mission as the sensitivity requirements lead to the need to maximize the size of the FOV while fitting within the tight mass and size constraints imposed by a space mission. Given the heritage of past satellite missions it will be possible to develop a telescope design that meets the requirements for a future mission and uses high TRL components.

Optical Coupling: The need for sensitivity drives the push for high efficiency optics; wide bandwidth to compliment mutichroic detector ; infrared filters to maximize cryogenic performance; and polarization modulators to suppress $1/f$ noise and mitigate instrument systematics. The CMB field has made tremendous progress recently by drawing on advances in materials, processing techniques, and developments in electrical engineering including meta-material research. Single crystals such as silicon and sapphire are attractive since they offer extremely low dielectric losses and high indices of refraction to better manipulate light. New coating techniques have been developed for silicon and sapphire that span 2:1 bandwidth (TRL 5+ for silicon) and can realize up to 5:1 bandwidth. EBEX deployed broadband cryogenic polarization modulator with a superconducting bearing that covered 150 GHz band to 410 GHz band raising the modulators to TRL 5+ for space. Meta-material metal-mesh optical filters were deployed with the Planck satellite and they are extensively used by ground based and balloon experiments making these TRL6 optical elements. It is necessary to develop a plan for a satellite mission that will cover $\sim$ 30 GHz to $\sim$ 800 GHz. Two

configurations could be considered: multiple optical paths with $< 3:1$ bandwidth and a potentially simpler design with only two optical paths with $\sim 5:1$ bandwidth. These studies include evaluating the design tradeoffs inherent to these approaches, developing the new coatings needed, and evaluating the promise of hybrid approaches where filters and lenses are implemented in the same optical elements. In addition, the cryogenic rotation mechanism should be demonstrated at the robustness (eg lifetime) needed for for a satellite mission.

Detector Coupling: The focal-plane feed determines the shape and polarization properties of the pixel beams and therefore plays a strong role in controlling systematic errors. The feed design also can determine the total bandwidth and number of photometric bands of each pixel which is important for the efficient use of a telescope's focal plane area. CMB experiments developed broadband multi-chroic *detector* to increase optical throughput of a focal plane. Broadband feed captures signal over wide frequency range. Then on-chip superconducting filter partitions signal into multiple frequency bands prior to detection. Broadband detectors were realized with spline profiled horn and lenslet coupled antenna. Broadband horn detector deployed a pixel that covers 2.3:1 bandwidth with on going development for extending bandwidth to 6:1. Broadband lenslet coupled antenna will deploy 3:1 bandwidth detector this year. Lenslet coupled antenna demonstrated 5:1 bandwidth in laboratory. RF-techniques to partition broadband signals into multiple band are mature. For a future CMB polarization satellite mission, broadband feed should be demonstrated at high frequency where alignment and line width for micro-fabrication becomes challenging. Detectors for CMB satellite mission were hand picked one by one for optimal performance. Next generation of detector array will be fabricated on a silicon wafer. Micro-fabrication process should demonstrate high yield and uniformity across a wafer that can meet tight requirement of satellite mission. Also detector test need to able to characterize detector beyond the level of systematic required by next generation CMB satellite experiment.

The Planck HFI deployed Neutron Transmutation Doped Germanium high-resistance bolometer at 100 milli-Kelvin to achieve photon noise limited detector performance. A Transition Edge Sensor (TES) bolometer uses a steep transition of superconducting metal to improve linearity of the detector. TES bolometers have been deployed on 100 milli-Kelvin and 250 milli-Kelvin platform. TES bolometers have been deployed across ground based and balloon CMB experiments spanning 40 GHz-410 GHz with detectors achieving NEPs of 20-50 aW/$\sqrt{\text{Hz}}$, nearly background limited at CMB frequencies. TES bolometers deployed at low optical frequencies ($\sim$40 GHz) and balloon-borne payloads should realized even lower NEPs of $\sim$10 aW/$\sqrt{\text{Hz}}$. Emerging detector technology for CMB experiment is kinetic-inductance detector (KIDs). The KIDs detector detects signal as change in kinetic inductance. KIDs detectors can be frequency multiplexed easily to $\sim 1,000$ detectors. Recently, on-sky demonstration at 150 GHz and 230 GHz was done with lumped element KID detector. Noise performance of KID detector at low frequency channels (< 40 GHz) need some improvement to be photon-noise limited. Currently there is no CMB polarizatin power spectrum data produced with KID detector. Coupling between RF (100 GHz) signal to micro-wave KID (MKID) detector is in a development stage. Planck detectors experienced unexpectedly high rate of cosmic ray events. Data was successfully cleaned with analysis technique. Study of impact of cosmic rays on a detector is crucial for next CMB satellite mission.

Multiplexed readout is being used by CMB experiments to readout thousands of TES bolometers, and readout multiplexing is built into KID detector architecture. Voltage bias and low impedance of a TES bolometer facilitates multiplexing readout by Superconducting Quantum Interference De-

vice (SQUID). Time domain multiplexing uses a SQUID at milli-Kelvin as a switch to rapidly cycle through bolometers. Highest achieved multiplexing factor is 64 channels. Frequency domain multiplexing uses superconducting resonators to assign bolometers to different frequency channels. Highest achieved multiplexing factor is 68 channels. New readout scheme, such as microwave SQUID readout, is emerging to increase multiplexing factor for TES bolometer. MKID detector architecture has multiple resonators coming off from a transmission line. A resonator is both a detector and multiplexer. MKID demonstrated multiplexing factor that exceeds 1,000 channels. For next generation satellite experiment that will readout over thousands detectors require high multiplexing factor. Multiplexing factor is directly related to readout complexity and power consumption. Also the Planck mission experienced ADC non-linearity, thus extensive characterization of end to end readout archtecture should be performed pre-flight.

A future CMB satellite mission offers exciting opportunity for millimeter wave polarization science. Experience from Planck mission will be studied to learn lessons for the future mission. Development for CMB instrumentation is an active field with many institutions developing new technologies for ground based, balloon, and proposed satellite missions. For a satellite instrumentation, there is a difficult trade off between desire to have high performance instrument and desire to keep cost manageable. Many developments that is going on for ground based and balloon experiment have similar goal as satellite mission that collaborative development across all platform will be beneficial.

1.6 Mission Study, and Management Plan

1.5 pages; Describe what we want to do, who is doing what, what we are funding

Shaul is writing this. Due by Tuesday Nov. 1

References

[1] A. H. Guth. Inflationary universe: A possible solution to the horizon and flatness problems. *Phys. Rev. D.*, 23:347–356, January 1981.

[2] A. D. Linde. A New Inflationary Universe Scenario: A Possible Solution of the Horizon, Flatness, Homogeneity, Isotropy and Primordial Monopole Problems. *Phys. Lett.*, B108:389–393, 1982.

[3] A. Albrecht and P. J. Steinhardt. Cosmology for grand unified theories with radiatively induced symmetry breaking. *Phys. Rev. Lett.*, 48:1220–1223, 1982.

[4] K. Sato. First-order phase transition of a vacuum and the expansion of the Universe. *MNRAS*, 195:467–479, May 1981.

[5] E. W. Kolb and M. S. Turner. *The Early Universe*. Addison-Wesley, Redwood City, CA, 2nd. edition, 1994.

[6] D. N. Spergel, R. Bean, O. Doré, M. R. Nolta, C. L. Bennett, J. Dunkley, G. Hinshaw, N. Jarosik, E. Komatsu, L. Page, H. V. Peiris, L. Verde, M. Halpern, R. S. Hill, A. Kogut, M. Limon, S. S. Meyer, N. Odegard, G. S. Tucker, J. L. Weiland, E. Wollack, and E. L. Wright. Three-Year Wilkinson Microwave Anisotropy Probe (WMAP) Observations: Implications for Cosmology, June 2007.

[7] M. Tegmark, D. Eisenstein, M. Strauss, D. Weinberg, M. Blanton, J. Frieman, M. Fukugita, J. Gunn, A. Hamilton, G. Knapp, R. Nichol, J. Ostriker, N. Padmanabhan, W. Percival, D. Schlegel, D. Schneider, R. Scoccimarro, U. Seljak, H. Seo, M. Swanson, A. Szalay, M. Vogeley, J. Yoo, I. Zehavi, K. Abazajian, S. Anderson, J. Annis, N. Bahcall, B. Bassett, A. Berlind, J. Brinkmann, T. Budavari, F. Castander, A. Connolly, I. Csabai, M. Doi, D. Finkbeiner, B. Gillespie, K. Glazebrook, G. Hennessy, D. Hogg, Z. Ivezic, B. Jain, D. Johnston, S. Kent, D. Lamb, B. Lee, H. Lin, J. Loveday, R. Lupton, J. Munn, K. Pan, C. Park, J. Peoples, J. Pier, A. Pope, M. Richmond, C. Rockosi, R. Scranton, R. Sheth, A. Stebbins, C. Stoughton, I. Szapudi, D. Tucker, D. Vanden Berk, B. Yanny, and D. York. Cosmological Constraints from the SDSS Luminous Red Galaxies. *Phys. Rev. D.*, 74:123507, 2006.

[8] Planck Collaboration, P. A. R. Ade, N. Aghanim, M. Arnaud, M. Ashdown, J. Aumont, C. Baccigalupi, A. J. Banday, R. B. Barreiro, J. G. Bartlett, and et al. Planck 2015 results. XIII. Cosmological parameters. *ArXiv e-prints*, February 2015.

[9] Planck Collaboration, P. A. R. Ade, N. Aghanim, M. Arnaud, F. Arroja, M. Ashdown, J. Aumont, C. Baccigalupi, M. Ballardini, A. J. Banday, and et al. Planck 2015. XX. Constraints on inflation. *ArXiv e-prints*, February 2015.

[10] M. Kamionkowski, A. Kosowsky, and A. Stebbins. A Probe of Primordial Gravity Waves and Vorticity. *Phys. Rev. Lett.*, 78:2058–2061, March 1997. astro-ph/9609132.

[11] M. Zaldarriaga and U. Seljak. All-sky analysis of polarization in the microwave background. *Phys. Rev. D.*, 55:1830–1840, 1997.

[12] Committee for a Decadal Survey of Astronomy and Astrophysics. *New Worlds, New Horizons in Astronomy and Astrophysics*. National Academy Press, 2010.

[13] Viatcheslav Mukhanov. Quantum Cosmological Perturbations: Predictions and Observations. *Eur. Phys. J.*, C73:2486, 2013.

[14] Diederik Roest. Universality classes of inflation. *JCAP*, 1401:007, 2014.

[15] Paolo Creminelli, Sergei Dubovsky, Diana Lopez Nacir, Marko Simonovic, Gabriele Trevisan, Giovanni Villadoro, and Matias Zaldarriaga. Implications of the scalar tilt for the tensor-to-scalar ratio. *Phys. Rev.*, D92(12):123528, 2015.

[16] Ryo Namba, Marco Peloso, Maresuke Shiraishi, Lorenzo Sorbo, and Caner Unal. Scale-dependent gravitational waves from a rolling axion. *JCAP*, 1601(01):041, 2016.

[17] Marco Peloso, Lorenzo Sorbo, and Caner Unal. Rolling axions during inflation: perturbativity and signatures. 2016.

[18] Lawrence M. Krauss. Gravitational waves from global phase transitions. *Phys. Lett.*, B284:229–233, 1992.

[19] Katherine Jones-Smith, Lawrence M. Krauss, and Harsh Mathur. A Nearly Scale Invariant Spectrum of Gravitational Radiation from Global Phase Transitions. *Phys. Rev. Lett.*, 100:131302, 2008.

[20] John T. Giblin, Jr., Larry R. Price, Xavier Siemens, and Brian Vlcek. Gravitational Waves from Global Second Order Phase Transitions. *JCAP*, 1211:006, 2012.

[21] Daniel G. Figueroa, Mark Hindmarsh, and Jon Urrestilla. Exact Scale-Invariant Background of Gravitational Waves from Cosmic Defects. *Phys. Rev. Lett.*, 110(10):101302, 2013.

[22] Elisa Fenu, Daniel G. Figueroa, Ruth Durrer, Juan Garcia-Bellido, and Martin Kunz. Cosmic Microwave Background temperature and polarization anisotropies from the large-N limit of global defects. *Phys. Rev.*, D89(8):083512, 2014.

[23] Daniel Baumann and Matias Zaldarriaga. Causality and Primordial Tensor Modes. *JCAP*, 0906:013, 2009.

[24] Hayden Lee, S. C. Su, and Daniel Baumann. The Superhorizon Test of Future B-mode Experiments. *JCAP*, 1502(02):036, 2015.

[25] David H. Lyth. What would we learn by detecting a gravitational wave signal in the cosmic microwave background anisotropy? *Phys.Rev.Lett.*, 78:1861–1863, 1997.

[26] R. A. Sunyaev and Y. B. Zeldovich. The Spectrum of Primordial Radiation, its Distortions and their Significance. *Comments on Astrophysics and Space Physics*, 2:66, March 1970.

[27] C. Burigana. Distortions of the CMB Spectrum by Continuous Heating. In G. L. Chincarini, A. Iovino, T. Maccacaro, & D. Maccagni, editor, *Observational Cosmology*, volume 51 of *Astronomical Society of the Pacific Conference Series*, pages 554–+, January 1993.

[28] W. Hu and J. Silk. Thermalization and spectral distortions of the cosmic background radiation. *Phys. Rev. D.*, 48:485–502, July 1993.

[29] J. Chluba and R. A. Sunyaev. The evolution of CMB spectral distortions in the early Universe. *MNRAS*, 419:1294–1314, January 2012.

[30] J. C. Mather, E. S. Cheng, D. A. Cottingham, R. E. Eplee, Jr., D. J. Fixsen, T. Hewagama, R. B. Isaacman, K. A. Jensen, S. S. Meyer, P. D. Noerdlinger, S. M. Read, and L. P. Rosen. Measurement of the cosmic microwave background spectrum by the COBE FIRAS instrument. *Ap. J.*, 420:439–444, January 1994.

[31] D. J. Fixsen, E. S. Cheng, J. M. Gales, J. C. Mather, R. A. Shafer, and E. L. Wright. The Cosmic Microwave Background Spectrum from the Full COBE FIRAS Data Set. *Ap. J.*, 473:576–+, December 1996.

[32] J. Chluba. Which spectral distortions does ΛCDM actually predict? *MNRAS*, 460:227–239, July 2016.

[33] A. Kogut, D. J. Fixsen, D. T. Chuss, J. Dotson, E. Dwek, M. Halpern, G. F. Hinshaw, S. M. Meyer, S. H. Moseley, M. D. Seiffert, D. N. Spergel, and E. J. Wollack. The Primordial Inflation Explorer (PIXIE): a nulling polarimeter for cosmic microwave background observations. *JCAP*, 7:25–+, July 2011.

[34] P. André, C. Baccigalupi, A. Banday, D. Barbosa, B. Barreiro, J. Bartlett, N. Bartolo, E. Battistelli, R. Battye, G. Bendo, A. Beno#523t, J.-P. Bernard, M. Bersanelli, M. Béthermin, P. Bielewicz, A. Bonaldi, F. Bouchet, F. Boulanger, J. Brand, M. Bucher, C. Burigana, Z.-Y. Cai, P. Camus, F. Casas, V. Casasola, G. Castex, A. Challinor, J. Chluba, G. Chon, S. Colafrancesco, B. Comis, F. Cuttaia, G. D'Alessandro, A. Da Silva, R. Davis, M. de Avillez, P. de Bernardis, M. de Petris, A. de Rosa, G. de Zotti, J. Delabrouille, F.-X. Désert, C. Dickinson, J. M. Diego, J. Dunkley, T. Enßlin, J. Errard, E. Falgarone, P. Ferreira, K. Ferrière, F. Finelli, A. Fletcher, P. Fosalba, G. Fuller, S. Galli, K. Ganga, J. García-Bellido, A. Ghribi, M. Giard, Y. Giraud-Héraud, J. Gonzalez-Nuevo, K. Grainge, A. Gruppuso, A. Hall, J.-C. Hamilton, M. Haverkorn, C. Hernandez-Monteagudo, D. Herranz, M. Jackson, A. Jaffe, R. Khatri, M. Kunz, L. Lamagna, M. Lattanzi, P. Leahy, J. Lesgourgues, M. Liguori, E. Liuzzo, M. Lopez-Caniego, J. Macias-Perez, B. Maffei, D. Maino, A. Mangilli, E. Martinez-Gonzalez, C. Martins, S. Masi, M. Massardi, S. Matarrese, A. Melchiorri, J.-B. Melin, A. Mennella, A. Mignano, M.-A. Miville-Deschênes, A. Monfardini, A. Murphy, P. Naselsky, F. Nati, P. Natoli, M. Negrello, F. Noviello, C. O'Sullivan, F. Paci, L. Pagano, R. Paladino, N. Palanque-Delabrouille, D. Paoletti, H. Peiris, F. Perrotta, F. Piacentini, M. Piat, L. Piccirillo, G. Pisano, G. Polenta, A. Pollo, N. Ponthieu, M. Remazeilles, S. Ricciardi, M. Roman, C. Rosset, J.-A. Rubino-Martin, M. Salatino, A. Schillaci, P. Shellard, J. Silk, A. Starobinsky, R. Stompor, R. Sunyaev, A. Tartari, L. Terenzi, L. Toffolatti, M. Tomasi, N. Trappe, M. Tristram, T. Trombetti, M. Tucci, R. Van de Weijgaert, B. Van Tent, L. Verde, P. Vielva, B. Wandelt, R. Watson, and S. Withington. PRISM (Polarized Radiation Imaging and Spectroscopy Mission): an extended white paper. *JCAP*, 2:6, February 2014.

[35] Y. B. Zeldovich and R. A. Sunyaev. The Interaction of Matter and Radiation in a Hot-Model Universe. *ApSS*, 4:301–316, July 1969.

[36] R. A. Sunyaev and Y. B. Zeldovich. The interaction of matter and radiation in the hot model of the Universe, II. *ApSS*, 7:20–30, April 1970.

[37] R. A. Sunyaev and Y. B. Zeldovich. Formation of Clusters of Galaxies; Protocluster Fragmentation and Intergalactic Gas Heating. *Astron. Astrophys.*, 20:189–+, August 1972.

[38] W. Hu, D. Scott, and J. Silk. Reionization and cosmic microwave background distortions: A complete treatment of second-order Compton scattering. *Phys. Rev. D.*, 49:648–670, January 1994.

[39] S. P. Oh, A. Cooray, and M. Kamionkowski. Sunyaev-Zeldovich fluctuations from the first stars? *MNRAS*, 342:L20–L24, June 2003.

[40] R. Cen and J. P. Ostriker. Where Are the Baryons? *Ap. J.*, 514:1–6, March 1999.

[41] A. Refregier, E. Komatsu, D. N. Spergel, and U.-L. Pen. Power spectrum of the Sunyaev-Zel'dovich effect. *Phys. Rev. D.*, 61(12):123001, June 2000.

[42] J. C. Hill, N. Battaglia, J. Chluba, S. Ferraro, E. Schaan, and D. N. Spergel. Taking the Universe's Temperature with Spectral Distortions of the Cosmic Microwave Background. *Physical Review Letters*, 115(26):261301, December 2015.

[43] W. Hu and J. Silk. Thermalization constraints and spectral distortions for massive unstable relic particles. *Physical Review Letters*, 70:2661–2664, May 1993.

[44] J. Chluba. Distinguishing different scenarios of early energy release with spectral distortions of the cosmic microwave background. *MNRAS*, 436:2232–2243, December 2013.

[45] J. Chluba and D. Jeong. Teasing bits of information out of the CMB energy spectrum. *MNRAS*, 438:2065–2082, March 2014.

[46] E. Dimastrogiovanni, L. M. Krauss, and J. Chluba. Constraints on gravitino decay and the scale of inflation using CMB spectral distortions. *Phys. Rev. D.*, 94(2):023518, July 2016.

[47] K. Jedamzik, V. Katalinić, and A. V. Olinto. Limit on Primordial Small-Scale Magnetic Fields from Cosmic Microwave Background Distortions. *PRL*, 85:700–703, July 2000.

[48] H. Tashiro, E. Sabancilar, and T. Vachaspati. CMB distortions from superconducting cosmic strings. *Phys. Rev. D.*, 85(10):103522, May 2012.

[49] A. D. Dolgov and D. Ejlli. Resonant high energy graviton to photon conversion at the post-recombination epoch. *Phys. Rev. D.*, 87(10):104007, May 2013.

[50] H. Tashiro, J. Silk, and D. J. E. Marsh. Constraints on primordial magnetic fields from CMB distortions in the axiverse. *Phys. Rev. D.*, 88(12):125024, December 2013.

[51] R. R. Caldwell and N. A. Maksimova. Spectral distortion in a radially inhomogeneous cosmology. *Phys. Rev. D.*, 88(10):103502, November 2013.

[52] Y. Ali-Haïmoud, J. Chluba, and M. Kamionkowski. Constraints on Dark Matter Interactions with Standard Model Particles from Cosmic Microwave Background Spectral Distortions. *Physical Review Letters*, 115(7):071304, August 2015.

[53] R. A. Sunyaev and Y. B. Zeldovich. Small scale entropy and adiabatic density perturbations - Antimatter in the Universe. *ApSS*, 9:368–382, December 1970.

[54] R. A. Daly. Spectral distortions of the microwave background radiation resulting from the damping of pressure waves. *Ap. J.*, 371:14–28, April 1991.

[55] W. Hu, D. Scott, and J. Silk. Power spectrum constraints from spectral distortions in the cosmic microwave background. *Ap. J. Lett.*, 430:L5–L8, July 1994.

[56] J. Chluba, R. Khatri, and R. A. Sunyaev. CMB at 2 x 2 order: the dissipation of primordial acoustic waves and the observable part of the associated energy release. *MNRAS*, 425:1129–1169, September 2012.

[57] J. Chluba, A. L. Erickcek, and I. Ben-Dayan. Probing the Inflaton: Small-scale Power Spectrum Constraints from Measurements of the Cosmic Microwave Background Energy Spectrum. *Ap. J.*, 758:76, October 2012.

[58] J. B. Dent, D. A. Easson, and H. Tashiro. Cosmological constraints from CMB distortion. *Phys. Rev. D.*, 86(2):023514, July 2012.

[59] S. Clesse, B. Garbrecht, and Y. Zhu. Testing inflation and curvaton scenarios with CMB distortions. *JCAP*, 10:046, October 2014.

[60] G. Cabass, A. Melchiorri, and E. Pajer. μ distortions or running: A guaranteed discovery from CMB spectrometry. *Phys. Rev. D.*, 93(8):083515, April 2016.

[61] R. A. Sunyaev and J. Chluba. Signals from the epoch of cosmological recombination (Karl Schwarzschild Award Lecture 2008). *Astronomische Nachrichten*, 330:657–+, 2009.

[62] J. Chluba and Y. Ali-Haïmoud. COSMOSPEC: fast and detailed computation of the cosmological recombination radiation from hydrogen and helium. *MNRAS*, 456:3494–3508, March 2016.

[63] Planck Collaboration, P. A. R. Ade, N. Aghanim, C. Armitage-Caplan, M. Arnaud, M. Ashdown, F. Atrio-Barandela, J. Aumont, C. Baccigalupi, A. J. Banday, and et al. Planck 2013 results. XX. Cosmology from Sunyaev-Zeldovich cluster counts. *Astron. Astrophys.*, 571:A20, November 2014.

[64] S. Y. Sazonov and R. A. Sunyaev. Cosmic Microwave Background Radiation in the Direction of a Moving Cluster of Galaxies with Hot Gas: Relativistic Corrections. *Ap. J.*, 508:1–5, November 1998.

[65] N. Itoh, Y. Kohyama, and S. Nozawa. Relativistic corrections to the sunyaev-zeldovich effect for clusters of galaxies. *Ap. J.*, 502:7, July 1998.

[66] A. Challinor and A. Lasenby. Relativistic corrections to the sunyaev-zeldovich effect. *Ap. J.*, 499:1, May 1998.

[67] E. Pajer and M. Zaldarriaga. New Window on Primordial Non-Gaussianity. *Physical Review Letters*, 109(2):021302, July 2012.

[68] J. Ganc and E. Komatsu. Scale-dependent bias of galaxies and μ-type distortion of the cosmic microwave background spectrum from single-field inflation with a modified initial state. *Phys. Rev. D.*, 86(2):023518, July 2012.

[69] M. Biagetti, H. Perrier, A. Riotto, and V. Desjacques. Testing the running of non-Gaussianity through the CMB μ-distortion and the halo bias. *Phys. Rev. D.*, 87(6):063521, March 2013.

[70] R. Emami, E. Dimastrogiovanni, J. Chluba, and M. Kamionkowski. Probing the scale dependence of non-Gaussianity with spectral distortions of the cosmic microwave background. *Phys. Rev. D.*, 91(12):123531, June 2015.

[71] J. A. Rubiño-Martín, C. Hernández-Monteagudo, and R. A. Sunyaev. The imprint of cosmological hydrogen recombination lines on the power spectrum of the CMB. *Astron. Astrophys.*, 438:461–473, August 2005.

[72] C. Hernández-Monteagudo, J. A. Rubiño-Martín, and R. A. Sunyaev. On the influence of resonant scattering on cosmic microwave background polarization anisotropies. *MNRAS*, 380:1656–1668, October 2007.

[73] A. Lewis. Rayleigh scattering: blue sky thinking for future CMB observations. *JCAP*, 8:053, August 2013.

[74] K. Basu, C. Hernández-Monteagudo, and R. A. Sunyaev. CMB observations and the production of chemical elements at the end of the dark ages. *Astron. Astrophys.*, 416:447–466, March 2004.

[75] D. R. G. Schleicher, D. Galli, F. Palla, M. Camenzind, R. S. Klessen, M. Bartelmann, and S. C. O. Glover. Effects of primordial chemistry on the cosmic microwave background. *Astron. Astrophys.*, 490:521–535, November 2008.

[76] Planck Collaboration, R. Adam, P. A. R. Ade, N. Aghanim, M. Arnaud, J. Aumont, C. Baccigalupi, A. J. Banday, R. B. Barreiro, J. G. Bartlett, and et al. Planck intermediate results. XXX. The angular power spectrum of polarized dust emission at intermediate and high Galactic latitudes. *ArXiv e-prints*, September 2014.

[77] Planck Collaboration, P. A. R. Ade, N. Aghanim, C. Armitage-Caplan, M. Arnaud, M. Ashdown, F. Atrio-Barandela, J. Aumont, C. Baccigalupi, A. J. Banday, and et al. Planck 2013 results. XVIII. The gravitational lensing-infrared background correlation. *Astron. Astrophys.*, 571:A18, November 2014.

[78] P. Madau and M. Dickinson. Cosmic Star-Formation History. *ARA&A*, 52:415–486, August 2014.

[79] L. Wang, M. Viero, N. P. Ross, V. Asboth, M. Béthermin, J. Bock, D. Clements, A. Conley, A. Cooray, D. Farrah, A. Hajian, J. Han, G. Lagache, G. Marsden, A. Myers, P. Norberg, S. Oliver, M. Page, M. Symeonidis, B. Schulz, W. Wang, and M. Zemcov. Co-evolution of black hole growth and star formation from a cross-correlation analysis between quasars and the cosmic infrared background. *MNRAS*, 449:4476–4493, June 2015.

[80] P. Serra, G. Lagache, O. Doré, A. Pullen, and M. White. Cross-correlation of cosmic far-infrared background anisotropies with large scale structures. *Astron. Astrophys.*, 570:A98, October 2014.

[81] M. Fornasa, A. Cuoco, J. Zavala, J. M. Gaskins, M. A. Sanchez-Conde, G. Gomez-Vargas, E. Komatsu, T. Linden, F. Prada, F. Zandanel, and A. Morselli. The angular power spectrum of the diffuse gamma-ray emission as measured by the Fermi Large Area Telescope and constraints on its Dark Matter interpretation. *ArXiv e-prints*, August 2016.

[82] C. Feng, A. Cooray, and B. Keating. Planck Lensing and Cosmic Infrared Background Cross-Correlation with Fermi-LAT: Tracing Dark Matter Signals in the γ-ray Background. *ArXiv e-prints*, August 2016.

[83] B. D. Sherwin and M. Schmittfull. Delensing the CMB with the cosmic infrared background. *Phys. Rev. D.*, 92(4):043005, August 2015.

[84] P. Larsen, A. Challinor, B. D. Sherwin, and D. Mak. Demonstration of cosmic microwave background delensing using the cosmic infrared background. *ArXiv e-prints*, July 2016.

[85] Planck Collaboration, N. Aghanim, M. Arnaud, M. Ashdown, J. Aumont, C. Baccigalupi, A. J. Banday, R. B. Barreiro, J. G. Bartlett, N. Bartolo, and et al. Planck 2015 results. XI. CMB power spectra, likelihoods, and robustness of parameters. *Astron. Astrophys.*, 594:A11, September 2016.

2 Curriculum Vitae

3 Summary of Work Effort

4 Current and Pending Support

5 Letters of Support

6 Budget Details - Narrative

6.1 Team, and Work Effort

6.1.1 Funded Team Members

6.1.2 Non-Funded Team Members

6.2 Costing Principles

- **Summer Salaries:**
  - **Workshop:**

6.3 University of Minnesota Budget

6.3.1 Direct Labor

6.3.2 Supplies

6.3.3 Travel

6.3.4 Other Direct Costs

Publications and Teleconferencing
Other Subcontracts

6.3.5 Facilities and Administrative Costs

7 Budget Sheets

ACS attitude control system

ADC analog-to-digital converters

ADS attitude determination software

AHWP achromatic half-wave plate

AMC Advanced Motion Controls

ARC anti-reflection coatings

ATA advanced technology attachment

BRC bolometer readout crates

BLAST Balloon-borne Large-Aperture Submillimeter Telescope

CANbus controller area network bus

CMB cosmic microwave background

CMM coordinate measurement machine

CSBF Columbia Scientific Balloon Facility

CCD charge coupled device

DAC digital-to-analog converters

DASI Degree Angular Scale Interferometer

dGPS differential global positioning system

DfMUX digital frequency domain multiplexer

DLFOV diffraction limited field of view

DSP digital signal processing

EBEX E and B Experiment

EBEX2013 EBEX2013

ELIS EBEX low inductance striplines

ETC EBEX test cryostat

FDM frequency domain multiplexing

FPGA field programmable gate array

FCP flight control program

FOV field of view

FWHM full width half maximum

GPS global positioning system

HDPE high density polyethylene

HIM high index materials

HWP half-wave plate

IA integrated attitude

IP instrumental polarization

JSON JavaScript Object Notation

LDB long duration balloon

LED light emitting diode

LCS liquid cooling system

LC inductor and capacitor

LZH Lazer Zentrum Hannover

MCP multi-color pixel

MSM millimeter and sub-millimeter

MLR multilayer reflective

MAXIMA Millimeter Anisotropy eXperiment IMaging Array

NASA National Aeronautics and Space Administration

NDF neutral density filter

PCB printed circuit board

PE polyethylene

PME polarization modulation efficiency

PSF point spread function

PV pressure vessel

PWM pulse width modulation

RMS root mean square

SLR single layer reflective

SMB superconducting magnetic bearing

SQUID superconducting quantum interference device

SQL structured query language

STARS star tracking attitude reconstruction software

SWS sub-wavelength structures

TES transition edge sensor

TDRSS tracking and data relay satellites

TM transformation matrix

UHMWPE ultra high molecular weight polyethylene

UMN University of Minnesota